CHAUTRU, J.-M., MOREL, Y. and HERROUIN, G. Geostatistical simulation of a commercial polymetallic nodule mining site. APCOM 87. Proceedings of the Twentieth International Symposium on the Application of Computers and Mathematics in the Mineral Industries. Volume 3: *Geostatistics*. Johannesburg, SAIMM, 1987. pp. 177 – 185.

Geostatistical Simulation of a Commercial Polymetallic Nodule Mining Site

J.-M. CHAUTRU*, Y. MOREL† and G. HERROUIN†

**Centre de Géostatistique, Fontainebleau, France*
†GEMONOD, Centre de Toulon de l'IFREMER, La Seyne, France

A geostatistical simulation of a typical mining site for polymetallic nodules in the North Pacific Ocean is presented. This is the first stage in the design of an industrial mining system.

Two variables which have a major effect on the orebody's economic potential are considered, namely: the maximum slope of the ground inside a mining block of 50 × 100 m; and the average quantity of nodules on the same support.

Two geostatistical problems have emerged in this study. The first is due to the lack of a change of support model for the maximum of a variable. A provisional solution, considering an experimentally accessible 'equivalent' support, is proposed. The second is due to a non-linear link between the two variables. To be able to take this into account in the simulation, we propose a new method based on the decomposition: X = E(X/Y) + Residue (X).

Satisfactory results were obtained with this approach.

Introduction

In this paper we present a geostatistical mining site simulation prepared for GEMONOD (Groupement pour la Mise au Point des Moyens Nécessaires à l'Exploitation des Nodules Polymétalliques). It represents the sea-floor slope and nodule abundance in a specific area in the North-East tropical Pacific Ocean.[1] This area is part of a zone for which AFERNOD (Association of IFREMER, IMETAL, CEA and NORMED for the future exploitation of nodules) has filed an application for a pioneer area to the Preparatory Commission for the International Authority of the Deep Sea Bed.

The simulation is presently used to design an industrial mining system for polymetallic nodules.

We first show the place of this work in the whole project, and discuss the choice of the variables and the characteristics of the simulation. Then, after a quick overview of the prospection data, we present the geostatistical analysis and the simulation of the mining site.

Purpose and characteristics of the simulation

Designing an industrial nodule mining system requires a fairly good knowledge of the environmental constraints that this system will have to cope with. The operational performances of a given system will depend on its sensitivity to a variety of parameters describing the mining site. These parameters are numerous. Some of them must obviously be studied and modelled in detail. The most sensitive of them are those whose natural variations have a strong influence on the overall performance of the mining

system. For example, among the weather and sea-state conditions, wind speed and direction are determining factors.

As for the geological factors which interest us here, nodule abundance, sea-floor slope and soil mechanical properties are important, because they are limiting factors for the mining lane definition. More precisely because of its size, its weight, its power and its stability, the miner cannot move if the soil is too soft, or if the slope is too big (we assume over 10% in this study). Moreover, the trafficable areas must bear enough nodules to be mined.

That is why it is important to have an image of the spatial distribution of these variables. This image is given by the geostatistical simulation of nodule abundance and sea-floor slope. The data on the shear strength are too sparse at present to allow a good study.

In practice, we have produced a 2-D regular grid of 450 × 500 points. Each node is the center of a simulated block of 50×100 m. This block size is a compromise between the maximum number of grid points to be computed, the size of the site to be modelled, the effective width of the bottom collector system (10 to 20 meters) and the spatial resolution of the abundance observations (20 to 30 meters).

This simulation is the cornerstone of mining strategy studies. [2 3 4] Particularly it is used for predicting the performance of a mining system, given its characteristics and a certain mining strategy, for example, for computing the efficiency of the system, which compares the weight of the collected nodules to the weight of the existing nodules on the mined areas. It is also indispensable for determining the characteristics of the exploited area (length and width of the mining lanes, and consequently frequency of manoeuvres, wasted time, etc.).

The prospection data

A computer file has been constructed from a detailed interpretation of the data collected by 20 of the 68 deep-towed photographic and microtopographic surveys of the IFREMER's Raie-2 and Epaulard systems.

The nodule abundance in kilograms per square meter and the slope of the sea floor in percent along the navigation track of the deep towed devices have been calculated from these data. Then we have built varying sized samples, within which the two variables are constant (Figure 1). This particularity will oblige us to weight all statistics (histograms, variograms, etc.) by sample length.

In the present work, seven of the twenty surveys have been selected, totalling 224 kilometers of track line, that represent one type of abundance and slope distribution, which is hopefully representative of a mineable area. More details have been published elsewhere. [1 5 6]

In addition to this, we used two other kinds of information:

(a) Sea-depth measurements obtained by sea-beam [7], and plotted on a regular grid with a mesh of 250 meters, and covering a large area. These data give us a good knowledge of the regional topographic structure of the mining site, which is characterized by an alternance of hills and valleys oriented roughly N-S. The anisotropy is very strong [1] and will be very important during the geostatistical study.

(b) Images collected with IFREMER's SAR system [8] which is a side-looking sonar capable of working down to a depth of 6000 meters. These images show topographic trends and details which are not detected by the sea-beam.

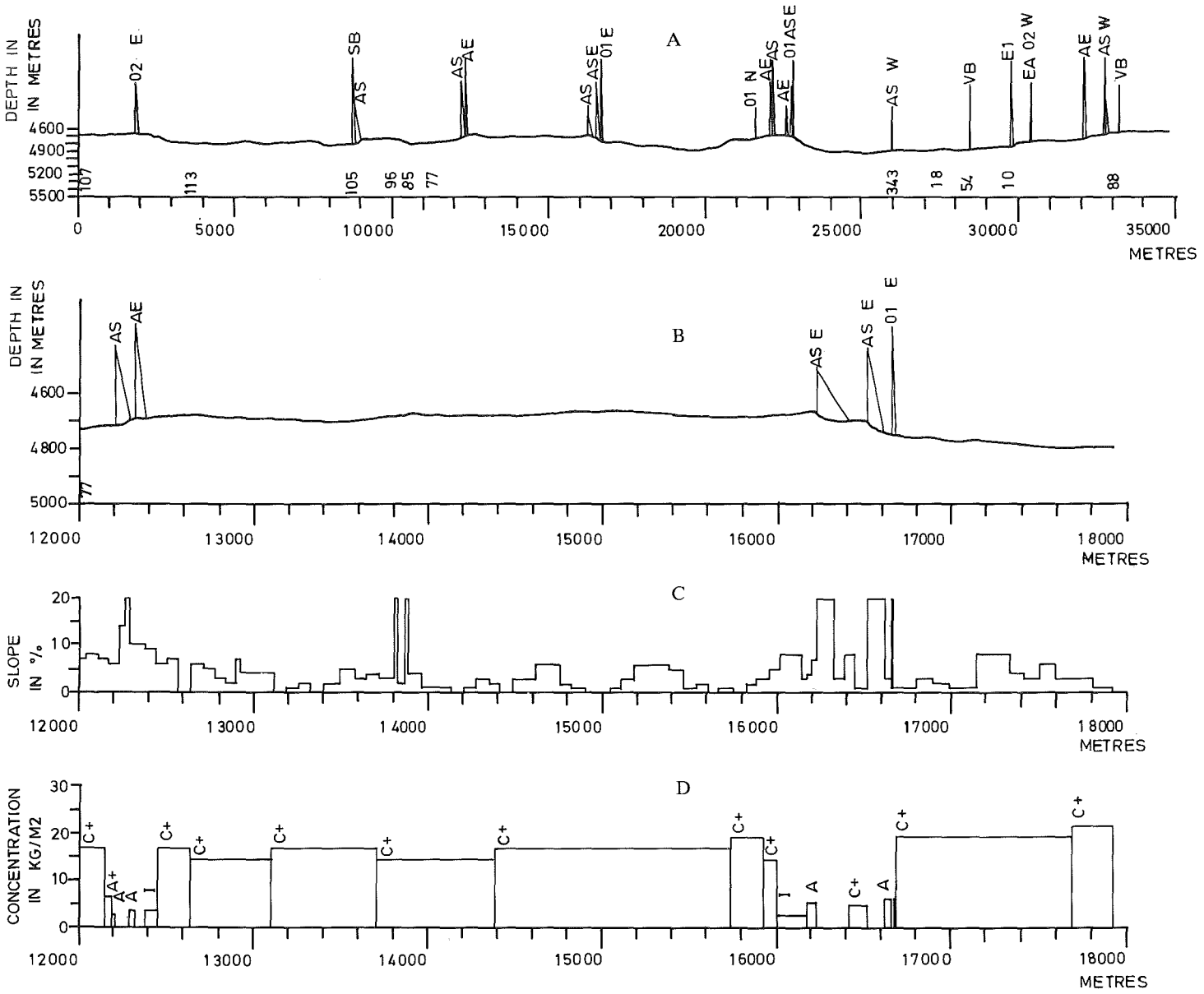

FIGURE 1. Graphic presentation of a photographic and microtopographic RAIE-2 survey.

A. *Depth variation in metres along the whole survey.* The vertical exaggeration is × 5. Between 0 and 15 000 metres, the abyssal hills are narrow and low. Beyond 15 000 metres, the hills become wider and higher. Obstacle photographic observations are reported along the depth line: AS, AE and AR as well as S, E and R are autocrops and blocks of sediments, polymetallic crusts and basaltic rocks. Small scarps are reported by their height in metres and their orientation: 02W is a two-metres high scarp facing west; scarps less than one metre high are reported as autocrops. Blocks are reported with their height: DA,; EB and D1 are encrusted blocks about 0,3, 0,6 and one metre high respectively. VB are whale bones. Numerical values over the abscissa line are headings of the track line

B. *Detail of a 6 km long portion of Figure 1A.* The vertical exaggeration is × 1.6 Note that the obstacles are generally clustered in sloped areas

C. *Slope variation of the sea bottom in percentage points over the same portion.* Slopes over 20% are cutoff. There is an average of one slope value every 80 metres.

D. *Nodule abundance variation in kg/m² over the same portion.* Where obstacles are observed, the abundance is zero, and abundance tends to drop in the vicinity of steep slopes and obstacles. There is an average of one abundance value every 260 metres

Geostatistical structural analysis

Data appraisal

Besides the varying sample size, numerical data coming from the system Raie-2 raise some difficulties.

The ground slope is the absolute difference of depth between the successive measurement points divided by their distance along the track line. This value is an oriented slope and does not represent the greatest dip at a given point, which interests the designer. In fact, because the topography is strongly oriented in the study area, these two slopes are approximately the same along the E-W track lines. But they are generally quite different along the other directions. Consequently, we can only consider the E-W slope data, and must use the sea-beam and SAR information for estimating the anisotropy. On the contrary, the nodule abundance data can be used along all directions.

Furthermore, we are only able to simulate 'Gaussian' (i.e. normally distributed) random functions. Then we have to anamorphosize (i.e. transform) the raw data to 'Gaussian' data. In the following sections, all the data are 'Gaussian', except where indicated.

Study of the slope

The main problem encountered in this study is the change of support, because we want to simulate 2-D blocks of 50 × 100 m with a non-regularizable variable. So we cannot use the usual change of support models. The designer is not interested in the mean slope of the block (how to define it?) but in the maximum dip value encountered in the block. If it is above a certain value, the block will be considered as dangerous and not mined.

No change of support model is available at present for the maximum value on a block. While waiting for the results of research on this subject, we propose the following intuitive approach:

We have noticed experimentally in 1-D that the moments of the maximum slope distribution, and the distribution itself, depend on the support. We can imagine that it varies with the slope's dispersion inside the support. In the 2-D case, we assume this distribution to be the same for two supports with the same dispersion variance, i.e. when

$\gamma(V_{1\text{-}D}, V_{1\text{-}D}) = \gamma(V_{2\text{-}D}, V_{2\text{-}D})$

γ is the point variogram of the slope (Fig. 2).

Then we determine experimentally a linear support 'equivalent' to the 50 × 100 m support. This length has been estimated at 58.6 m.

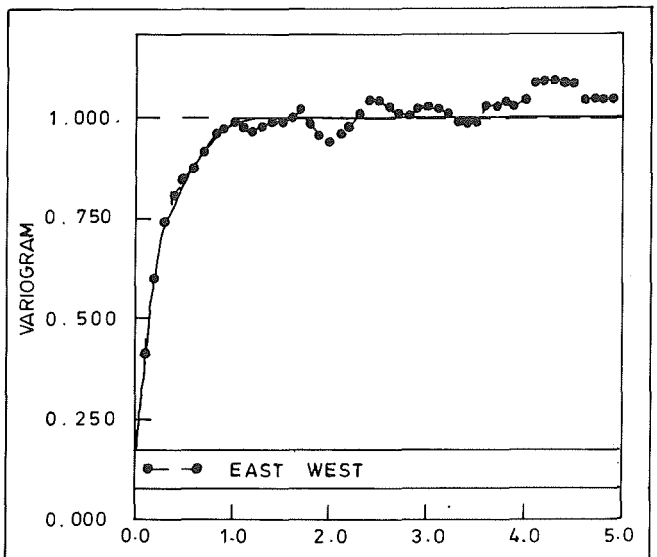

Distance in km

Model Fitted

Nugget effect = 0,08

+

3 spherical models:

Sill	*Range*	*Anisotropy*
0,47	300 m	EO:1 NS:0,26
0,21	950 m	– NS:0,13
0,24	1300 m	– NS:0,07

FIGURE 2. Punctual variogram of slope

The initial track lines are then cut into samples of 58.6 m, and the anamorphosis and the variogram to be used in the simulation are computed from these new data. Figures 3 and 4 show the histogram (for raw data) and the variogram (for Gaussian data) of maximum slope on a 58.6 m support together with their fitted models.

The anisotropy has been evaluated from a structural analysis of slopes computed from sea-beam data, and by observing the SAR images.

Correlation between slope and nodule abundance

These two variables must be studied on the same support. Then we have to regularize abundance on a 58.6 m support. But this length does not correspond to the 'equivalent' support of the 50 × 100 m block for nodule abundance, because the point variogram of this variable is different from the slope one. The Gaussian discretized model [9] shows the great similarity of the geostatistical characteristics for the two supports (Figures 5 and 6). Then we can work on the linear support and extend our conclusions to the rectangular one.

The correlation coefficient between the two variables is equal to -0.35. Figure 7 shows a non-linear relation between slope and nodule abundance. Note that a slight

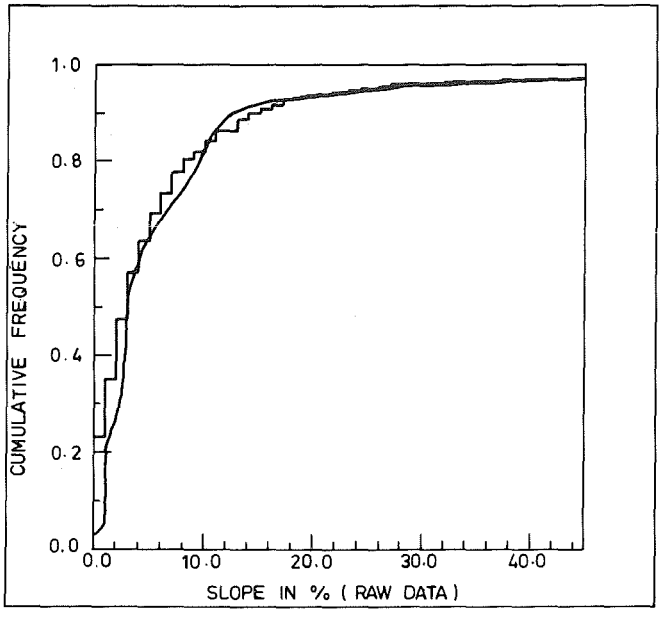

FIGURE 3. Histogram of slope on the linear support of 58,6 m

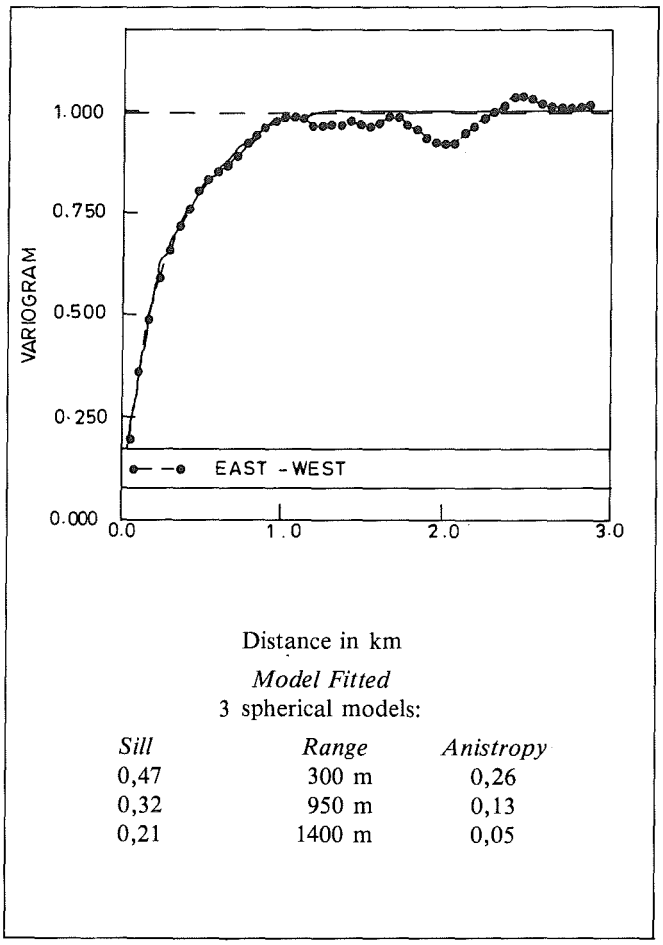

FIGURE 4. Variogram of slope on the linear support of 58,6 m

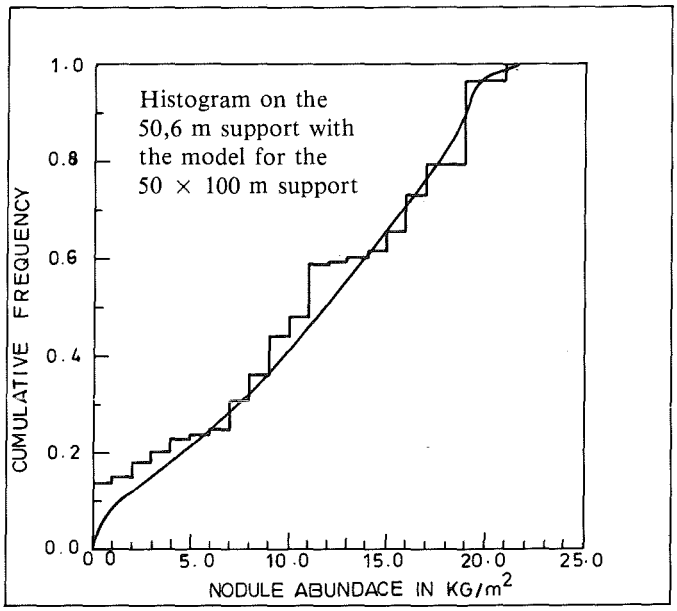

FIGURE 5. Histogram of nodule abundance on the 58,6 m support with the model for the 50 × 100 m support

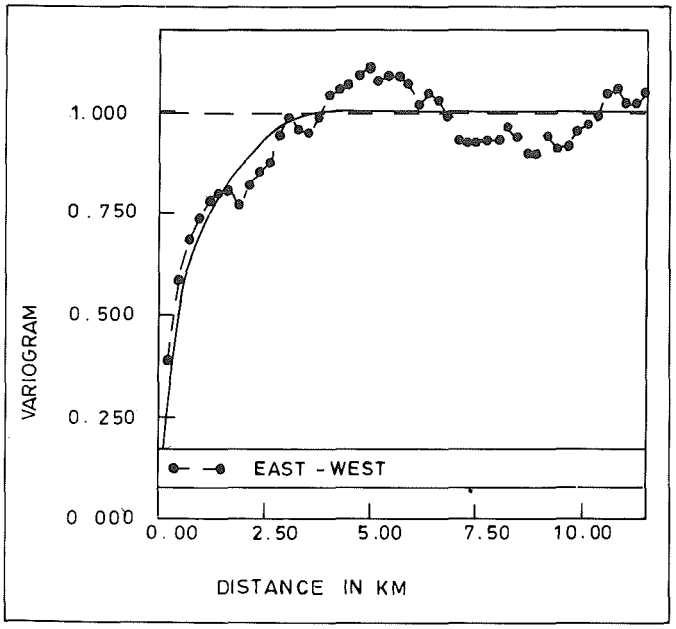

FIGURE 6. Variogram of nodule abundance on the 58,6 m support with the model for the 50 × 100 m support

slope is more favourable for abundance than flatness. We think that this geological fact is due to particular sedimentation conditions.

Because of the shape of the relation between the variables, we cannot carry out a bivariate simulation with usual models, but must find a new method to take this link into account.

We propose the following model:

$$X = E(X/Y) + Res(X)$$

with X = nodule abundance

Y = sea-floor maximum slope.

It is clear that, by construction, we have the following properties at a given point:

(a) E(X/Y) and Res(X) are uncorrelated;

(b) for a fixed Y, the mean of Res(X) is null.

Figure 8 shows that this last property is satisfied. Note that the oscillations are due to the fitting. Moreover, the correlation coefficient is equal to 0.01. On Figure 8, we can also see that, when Y is fixed, Var(E(X/Y)) is approximately constant except at the beginning of the curve, but this may be an artefact due to the very small number of data in the first classes of E(X/Y). Then we assume the independence between E(X/Y) and Res(X), at a given point.

Moreover, Figure 9 shows that these two variables are uncorrelated for two different points.

Finally, we assume independence between E(X/Y) and Res(X).

We can then simulate the nodule abundance as follows:

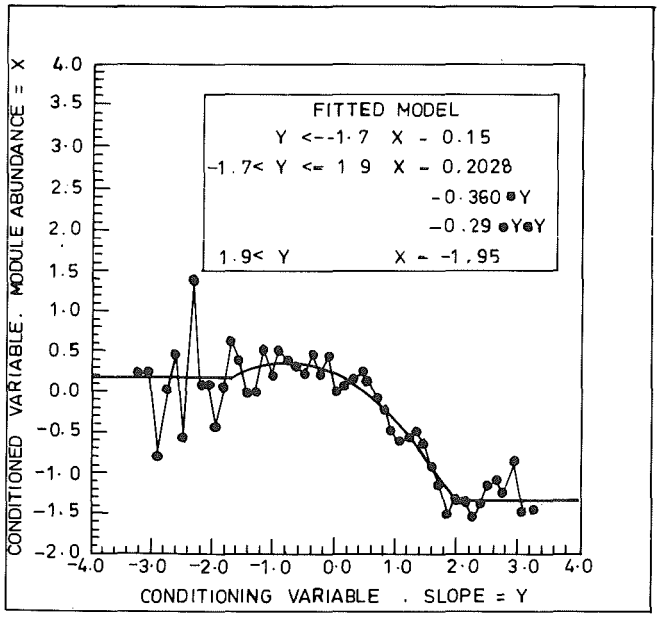

FIGURE 7. Experimental regression between abundance and slope

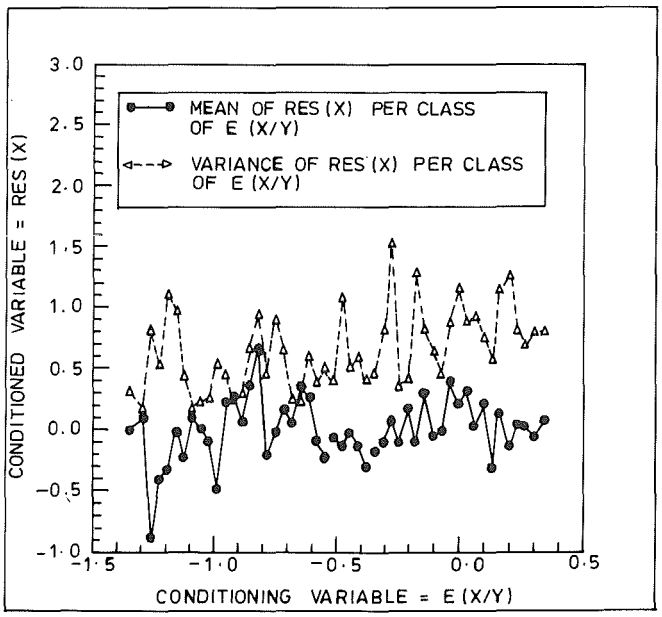

FIGURE 8. Experimental regression between RES(X) and E(X/Y)

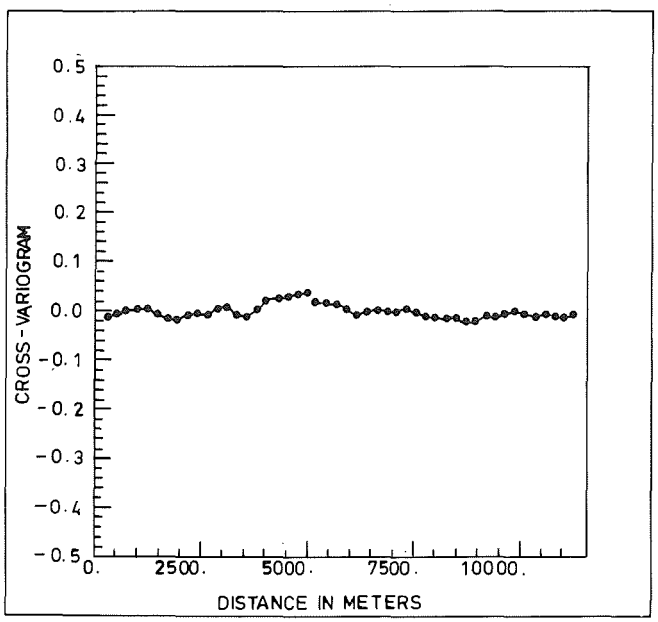

FIGURE 9. Cross-variogram between E(X/Y) and RES(X)

(a) computation of the expected value of abundance from the slope simulation by the fitted model of the regression curve (Figure 7);

(b) simulation of the residue Res(X);

(c) calculation of the final simulation as the sum of the previous ones;

(d) use of the anamorphosis function of nodule abundance to build the raw data simulation.

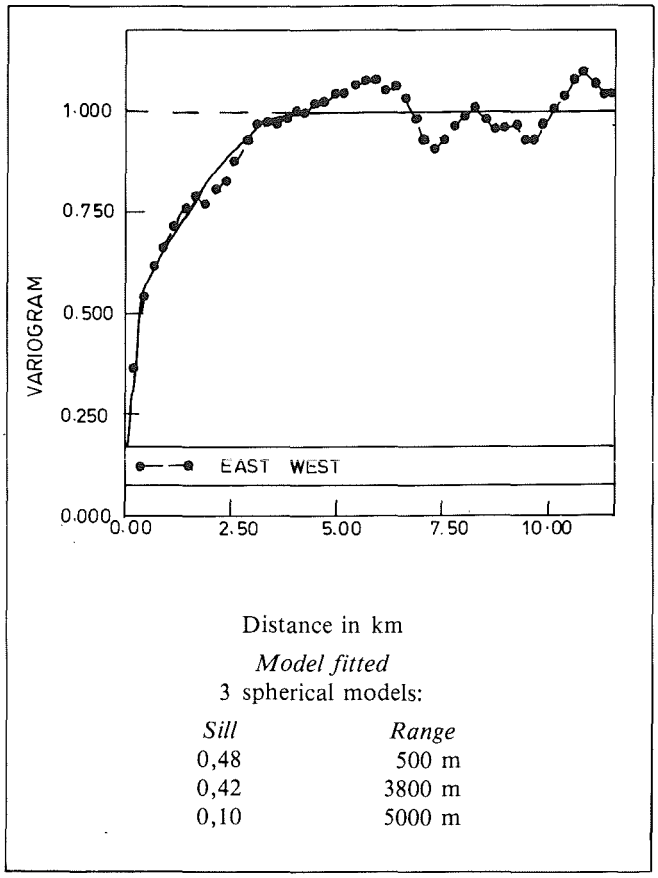

FIGURE 10. Variogram of the residue

The Raie-2 data study has shown that the nodule abundance was weakly anisotropic. Since Y and then E(X/Y) are strongly anisotropic, we have decided to consider the residue Res(X) as isotropic to compensate for the difference.

Figure 10 shows the variogram of the residue to be simulated.

Results of the simulation

The simulations of the slope and of the residue have been computed using the random tokens technique. On Figures 11 and 12, we can see examples of maps drawn from each final simulated grid, after being transformed back to raw data.

They represent the whole simulated area with a width of 22.5 km and a length of 50 km.

The link between the two variables has been respected, as are the variograms.[10]

Conclusion

These simulations have given good results, considered as realistic by the geologist. Since their variograms and histograms are similar to those of the presumed ore deposit, and since the relation between slope and concentration is respected, they make it possible to design the nodules mining system quite precisely. It is now possible to adapt the characteristics of the miner to the environmental conditions it will encounter.

This is a good example of the usefulness of geostatistical simulations.

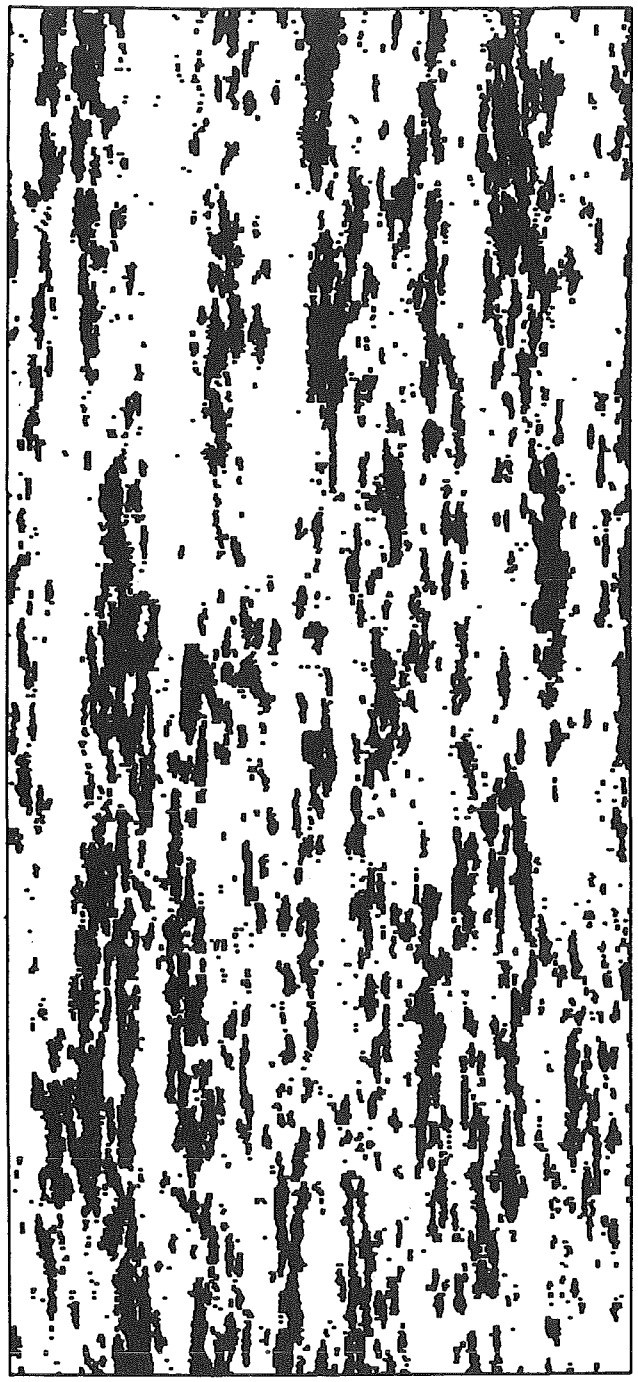

FIGURE 11. Map of the slope. On black areas the slope is over 10%

FIGURE 12. Map of nodule abundance. White areas represent rich zone, with a concentration over 10 kg/m^2

References

1. MOREL, Y. and LE SUAVE, R. l'environnement morphologique et sédimentaire dans un secteur intraplaque du Pacifique Nord (Zone Clarion-Clipperton). *Bull. Soc. Geol. de France*, t.II, n° 3, 1986, pp. 361-372.

2. CHARLES, C., TAINE, B. and SCHOENTGEN, P.A. Numerical study of the dynamic behaviour of a deep-sea mining system usig hydraulic lift. *Off-Shore Tech. Conf.*, 1986, Paper n° 5238.

3. CHARLES, C., CHASSERY, J.M. and MONTANVERT, A. Applications of image analysis to the determination of the

possible recovery system surveying patterns manganese nodules. *Off-Shore Tech. Conf.*, 1987, Paper n° 5473.

4. HERROUIN, G. and LE GOUELLEC, P. French program on polymetallic nodules deep-sea mining. *Proc. of the TECHNO-OCEAN '86 Symposium*, Kobé, Japan; 1986, pp. 10-31.
5. CHAUTRU, J.M. Etude structurale en vue d'une modélisation de gisement de nodules polymétalliques. *Sciences de la Terre, Série Inf. Géol*, Vol. 26.
6. MOREL, Y. and CHAUTRU, J.M. Essai de modélisation d'un site minier commercial à nodules polymétalliques. *Rev. Ind. Min., 'Les Techniques'*, Vol. 89, Février 1987.
7. RENARD, V. and ALLENOU, J.P. Sea-beam, multi-beam echo sounding in 'Jean-Charcot'. Description, evaluation and first results.
   Monaco, 1979, LVI(1).
8. FARCY, A. and ARZELIES, P. Connaissance des fonds sous-marins par imagerie acoustique. *Proc. of the 5th Congress of the Federation of the Acoustical Societies of Europe, FASE 87*, Lisbonne, 1987.
9. MATHERON, G. L'estimation globale des réserves récupérables.
   C-75, 1978.
10. CHAUTRU, J.M. Régression non linéaire et simulation de gisements de nodules polymétalliques. *Sciences de la Terre, Série Inf. Géol.*, To be published in 1987.